

A COMPTON-THICK AGN AT $Z \sim 5$ IN THE 4 MS *CHANDRA* DEEP FIELD SOUTHR. GILLI¹, J. SU², C. NORMAN^{2,3}, C. VIGNALI⁴, A. COMASTRI¹, P. TOZZI⁵, P. ROSATI⁶, M. STIAVELLI³, W.N. BRANDT^{7,8}, Y.Q. XUE^{7,8}, B. LUO^{7,8}, M. CASTELLANO⁹, A. FONTANA⁹, F. FIORE⁹, V. MAINIERI⁶, A. PTAK¹⁰

ABSTRACT

We report the discovery of a Compton-thick Active Galactic Nucleus (AGN) at $z = 4.76$ in the 4 Ms *Chandra* Deep Field South. This object was selected as a *V*-band dropout in HST/ACS images and previously recognized as an AGN from optical spectroscopy. The 4 Ms *Chandra* observations show a significant ($\sim 4.2\sigma$) X-ray detection at the *V*-band dropout position. The X-ray source displays a hardness ratio of $HR=0.23 \pm 0.24$, which, for a source at $z \sim 5$, is highly suggestive of Compton-thick absorption. The source X-ray spectrum is seen above the background level in the energy range of $\sim 0.9 - 4$ keV, i.e., in the rest-frame energy range of $\sim 5 - 23$ keV. When fixing the photon index to $\Gamma = 1.8$, the measured column density is $N_H = 1.4_{-0.5}^{+0.9} \times 10^{24} \text{ cm}^{-2}$, which is Compton-thick. To our knowledge, this is the most distant heavily obscured AGN, confirmed by X-ray spectral analysis, discovered so far. The intrinsic (de-absorbed), rest-frame luminosity in the 2-10 keV band is $\sim 2.5 \times 10^{44} \text{ erg s}^{-1}$, which places this object among type-2 quasars. The Spectral Energy Distribution shows that massive star formation is associated with obscured black hole accretion. This system may have then been caught during a major co-eval episode of black hole and stellar mass assembly at early times. The measure of the number density of heavily obscured AGN at high redshifts will be crucial to reconstruct the BH/galaxy evolution history from the beginning.

Subject headings: galaxies: active — galaxies: high-redshift — X-rays: galaxies

1. INTRODUCTION

While optically bright quasars are the most spectacular expression of accretion onto supermassive black holes (SMBHs) at galaxy centers, it is widely believed that SMBHs grow most of their mass during obscured phases, in which the detection of the nuclear power becomes challenging (e.g., Fabian 1999). Large amounts of gas and dust are found to hide the majority of Active Galactic Nuclei (AGN) in the nearby and distant Universe, as demonstrated by deep and wide X-ray surveys over different sky fields (see e.g., Brandt & Hasinger 2005 for a review). From ~ 30 to $\sim 50\%$ of all AGN are believed to be obscured by extreme gas column densities above $N_H = \sigma_T^{-1} \sim 10^{24} \text{ cm}^{-2}$. These objects are dubbed “Compton-thick” and represent the most elusive members of the AGN population. The evidence for an abundant population of local Compton-thick objects is compelling: up to $\sim 50\%$ of nearby Seyfert 2s contain a Compton-thick nucleus (Risaliti et al. 1999; Akylas & Georgantopoulos

2009); about 50 objects - mostly local - have been certified as “bona-fide” Compton-thick AGN by X-ray spectral analysis (Comastri 2004).

Synthesis models of the X-ray background (XRB) suggest that Compton-thick AGN must be abundant at least up to $z \sim 1$ to explain the peak of the XRB at 30 keV (see e.g., Gilli et al. 2007; Treister et al. 2009, and references therein). A population of distant, Compton-thick AGN, as abundant as that predicted by XRB synthesis models, is also required to match the SMBH mass function measured in nearby galaxies with that of “relic” SMBHs grown by accretion (e.g., Marconi et al. 2004). In recent years it has been proposed that Compton-thick AGN represent a key phase of the BH/galaxy coevolution, during which the BH is producing most of its feedback into the host galaxy (e.g., Daddi et al. 2007; Menci et al. 2008), and it has also been suggested that their number density steeply increases with redshift (Treister et al. 2009).

The observation of heavily obscured AGN at high- z , $z \gtrsim 2 - 3$, remains challenging and it is very difficult to estimate their abundance since they produce only a small fraction of the XRB emission and are thus poorly constrained by synthesis models. Deep X-ray surveys have proven effective in revealing a few “bona fide” Compton-thick AGN at high- z . For instance, four such objects at $1.53 < z < 3.70$ have been discovered in the *Chandra/XMM* - Deep field South (CDFs; see Norman et al. 2002; Comastri et al. 2011; Feruglio et al. 2011). Other examples of candidate Compton-thick AGN at high- z have been reported (e.g., Tozzi et al. 2006; Polletta et al. 2008), even up to $z=5.8$ (Brandt et al. 2001), albeit with poorer X-ray photon statistics. Selection techniques based on the strength of the mid-IR emission with respect to the optical and X-ray emission have also been developed and applied to select large populations of candidate Compton-thick AGN up

Electronic address: roberto.gilli@oabo.inaf.it

¹ INAF - Osservatorio Astronomico di Bologna, via Ranzani 1, 40127, Bologna, Italy

² Department of Physics and Astronomy, Johns Hopkins University, Baltimore, MD 21218, USA

³ Space Telescope Science Institute, 3700 San Martin Drive, Baltimore, MD 21218, USA

⁴ Dipartimento di Astronomia, Università degli Studi di Bologna, Via Ranzani 1, 40127 Bologna, Italy

⁵ INAF - Osservatorio Astronomico di Trieste, via Tiepolo 11, 34131, Trieste, Italy

⁶ European Southern Observatory, Karl Schwarzschild Strasse 2, 85748 Garching bei Muenchen, Germany

⁷ Department of Astronomy and Astrophysics, Pennsylvania State University, University Park, PA 16802, USA

⁸ Institute for Gravitation and the Cosmos, Pennsylvania State University, University Park, PA 16802, USA

⁹ INAF - Osservatorio Astronomico di Roma, via Frascati 33, 00040 Monteporzio Catone, Italy

¹⁰ NASA/GSFC, Greenbelt, MD 20771, USA

to $z = 2 - 3$ (Daddi et al. 2007; Alexander et al. 2008a; Fiore et al. 2009; Bauer et al. 2010). Once more, however, the lack of X-ray spectra prevents an unambiguous determination of the absorbing column density, making the measurements by these works largely uncertain.

In this paper we report the discovery of a “bona-fide” Compton-thick AGN at $z=4.76$ in the 4 Ms CDFS. A concordance cosmology with $H_0 = 70 \text{ km s}^{-1} \text{ Mpc}^{-1}$, $\Omega_m = 0.27$, $\Omega_\Lambda = 0.73$ is adopted throughout this paper.

2. SOURCE SELECTION AND OBSERVATIONS

We searched for V -band dropout objects in the HST/ACS v2.0 data of GOODS-South (Giavalisco et al. 2004) associated with X-ray emission in the 4 Ms *Chandra* image. We used the V_{606} -dropout selection criteria from Oesch et al. (2007), which effectively pick sources at $4.7 < z < 5.7^{11}$. Details on the production of the V -dropout catalog are given in Su et al. (2011). Additionally, we required a stellarity parameter (CLASS_STAR) greater than 0.9 in the z_{850} band to choose point-like sources. This led to 21 star-like V_{606} -dropouts with $z_{850} < 25.5$, among which there are four $z \sim 5$ galaxies, eleven stars, three lower-redshift galaxies, and one $z \sim 5$ AGN, which is the only object detected in X-rays (XID403 in the 4 Ms CDFS catalog of Xue et al. 2011). The remaining two candidates have not been identified spectroscopically. The measured AB magnitudes of XID403 in ACS images are: $V_{606} = 26.84 \pm 0.10$, $i_{775} = 25.21 \pm 0.04$, $z_{850} = 25.05 \pm 0.04$. The 5σ detection limit in the B_{435} -band is 28.4 AB mag.

XID403 ($\alpha_{J2000}=03:32:29.29$, $\delta_{J2000}=-27:56:19.5$) was recognized as an AGN at $z = 4.76$ based on FORS-2 spectroscopy (Vanzella et al. 2006). Its optical spectrum exhibits a narrow ($\text{FWHM} \lesssim 1000 \text{ km s}^{-1}$) Ly α emission line and a broader ($\text{FWHM} \sim 2000 \text{ km s}^{-1}$) NV λ 1240 emission line, with an integrated flux similar to Ly α . A more recent spectrum with DEIMOS/Keck confirms both features (Coppin et al. 2009). The Spectral Energy Distribution of XID403 was published by Coppin et al. (2009). Based on a LABOCA detection at $870 \mu\text{m}$, they showed that this source is a bright submillimeter galaxy with $\text{SFR} \sim 1000 M_\odot \text{ yr}^{-1}$. A large reservoir of molecular gas ($\sim 1.6 \times 10^{10} M_\odot$) was also identified through CO(2-1) observations (Coppin et al. 2010).

We considered the same optical to mid-IR datasets used by Coppin et al. (2009) and improved on the SED by adding the detection at 1.1 mm by AzTec/ASTE ($f_{1.1\text{mm}} = 3.3 \pm 0.5 \text{ mJy}$; Scott et al. 2010) and the Y , J and K_s magnitudes from the deep NIR imaging by HAWK-I/VLT ($Y_{AB} = 24.56 \pm 0.12$, $J_{AB} = 24.37 \pm 0.14$, $K_{AB} = 24.03 \pm 0.20$; Castellano et al. 2010). This object is also detected (at $\sim 3\sigma$) at 1.4 GHz with a peak flux of $22.3 \mu\text{Jy}$ (N. Miller priv. comm). Unfortunately, it falls just outside the areas covered by the $16 \mu\text{m}$ Spitzer/IRS mosaic (Teplitz et al. 2011) and GOODS-Herschel (PI D. Elbaz). XID403 is not detected in the 3 Ms *XMM* image of the CDFS.

3. X-RAY DATA ANALYSIS

A total exposure of $\lesssim 4$ Ms has been accumulated on the CDFS as a result of $\lesssim 54$ individual observations with ACIS-I performed during three different time periods: ~ 0.8 Ms in 2000, ~ 1 Ms in 2007 and ~ 2 Ms in 2010. X-ray data products, including event files for each observation and also for the merged dataset are publicly available¹². In this paper we use the data products by Xue et al. (2011) who derived X-ray source catalogs from a full reprocessing and astrometric recalibration of the event files. We used CIAO v4.1 and the Ftools package¹³ to perform X-ray aperture photometry at the position of XID403. The separation between the optical and X-ray centroids is $\sim 0.4''$, which is well within the 1σ X-ray source positional uncertainty ($\sim 0.47''$). To maximize the S/N ratio, we measured the source counts in different bands within a small aperture of $3''$ radius, which encloses $\sim 50\%$ of the PSF at 1.5 keV at the source location (~ 8 arcmin off-axis). We measured 37.0 ± 8.7 net counts in the 0.9-4 keV band, corresponding to a $\sim 4.2\sigma$ detection¹⁴. We verified that similar results are obtained when using different local background regions. The hardness ratio, defined as $\text{HR} = (\text{H-S})/(\text{H+S})$, where S and H are the net counts observed in the 0.5-2 keV and 2-7 keV bands, respectively, is $\text{HR} = 0.23 \pm 0.24$ (not corrected for vignetting). This value, for an AGN at $z \sim 5$ with a standard intrinsic spectrum (i.e., $\Gamma = 1.8$) is highly suggestive of heavy obscuration. For comparison, an AGN at $z \sim 5$ with $N_H \lesssim 10^{23} \text{ cm}^{-2}$ is expected to have $\text{HR} \lesssim -0.35$ at the source position. We extracted the X-ray spectrum in the 0.5-7 keV band using the same $3''$ radius aperture and verified that below 0.9 keV and above 4 keV the source emission is indistinguishable from the background. The spectrum and response files were created using the `psextract` script in CIAO. Since `psextract` does not account for the PSF fraction when building up the effective area file, we multiplied the 0.5-2 keV and 2-10 keV fluxes as obtained from the spectral fit by a factor of 2 and 2.5, respectively, to recover the full aperture-corrected X-ray fluxes. We found consistent results either using spectral responses extracted from individual observations, or those obtained as an exposure-weighted mean over all individual responses. To double check the reliability of this procedure we also built spectral response files for one of the *Chandra* exposures (ObsID=8594) using the ACIS-Extract software (Broos et al. 2010) which allows proper construction of effective area files at any PSF fraction. Again, consistent results are found when using the ACIS-Extract responses. We analyzed the X-ray spectrum with XSPEC v11.3.2 using the Cash statistic (Cash 1979) to estimate the best-fit parameters. Errors are quoted at 1σ confidence level. We first fitted the data using a powerlaw spectrum modified by galactic absorption, which returns $\Gamma = -0.64^{+1.15}_{-0.73}$. We then used the `plcabs` model (Yaqoob 1997), which follows the propagation of X-ray photons within a uniform, spherical obscuring medium, accounting for both photoelectric absorption and Compton scattering. This model can be used in the case of heavy absorption (up to $5 \times 10^{24} \text{ cm}^{-2}$) and up to rest-frame energies of ~ 20 keV. When fixing the photon in-

¹¹ An object is defined as a V_{606} -dropout if $V_{606} - i_{775} > \min[1.5 + 0.9(i_{775} - z_{850}), 2]$, $V_{606} - i_{775} > 1.2$, $i_{775} - z_{850} < 1.3$, $S/N(z_{850}) > 5$ and $S/N(B_{435}) < 3$.

¹² <http://cxc.harvard.edu/cda/Contrib/CDFS.html>

¹³ <https://www.cfa.harvard.edu/~john/funtools>

¹⁴ XID403 has 82 ± 25 net counts in the 0.5-8 keV band (100% PSF) in Xue et al. (2011), in agreement with our estimate.

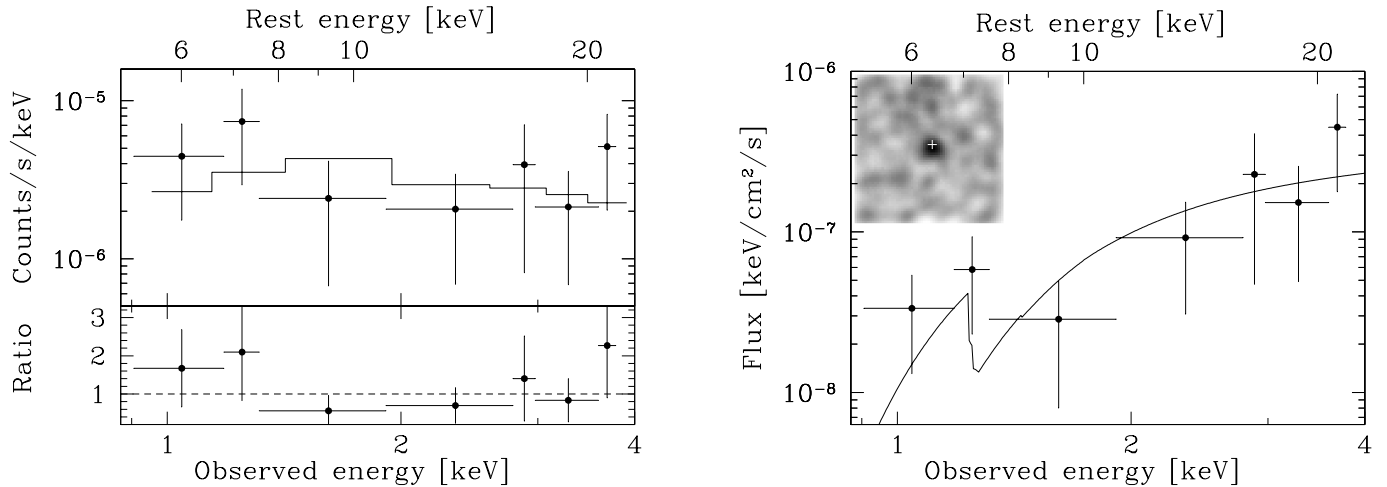


FIG. 1.— *Left*: The observed 4 Ms *Chandra* X-ray spectrum of XID403 and best-fit model (data/model ratio in the bottom panel). A best fit column density of $N_H = 1.4^{+0.9}_{-0.5} \times 10^{24} \text{ cm}^{-2}$ is obtained when assuming $\Gamma = 1.8$. The spectrum has been rebinned for display purposes. *Right*: Response corrected spectrum and best fit model. The inset shows a smoothed 0.9-4 keV image of XID403 (size is $30'' \times 30''$). The cross marks the position of the optical V-dropout.

dex to $\Gamma = 1.8$, we derived a Compton-thick column density of $N_H = 1.4^{+0.9}_{-0.5} \times 10^{24} \text{ cm}^{-2}$ (see Fig. 1). If we conservatively assume $\Gamma = 1.0$, which is $\gtrsim 4\sigma$ off the average intrinsic AGN value, we still obtain $N_H > 10^{24} \text{ cm}^{-2}$. The measured absorption should be interpreted as a lower limit, since a cold reflection model (*pexrav*), corresponding to $N_H \gtrsim 10^{25} \text{ cm}^{-2}$, provides an equally good fit.¹⁵ Fitting the data with the recent MYTorus model (Murphy & Yaqoob 2009), which accounts for a toroidal distribution of the obscuring matter, again returns $N_H > 10^{24} \text{ cm}^{-2}$. No prominent iron $K\alpha$ line is observed at 1.1 keV (i.e., 6.4 keV rest-frame), but this is not in conflict with the Compton-thick scenario. Indeed, the *observed* EW scales with $(1+z)^{-1}$, so that $\text{EW}_{rest} \sim 1\text{-}2 \text{ keV}$, as is typical of Compton-thick AGN, would translate into $\text{EW}_{obs} \sim 170\text{-}340 \text{ eV}$. We verified that such a weak line can be easily accommodated in the fit and that only loose upper limits can be derived for the equivalent width ($\text{EW}_{rest} < 4.3 \text{ keV}$ at 90% c.l.). The aperture-corrected X-ray fluxes, as extrapolated from the X-ray fit, are $f_{0.5-2} = 4.2 \pm 1.5 \times 10^{-17} \text{ erg cm}^{-2} \text{ s}^{-1}$ and $f_{2-10} = 6.8 \pm 2.4 \times 10^{-16} \text{ erg cm}^{-2} \text{ s}^{-1}$. The intrinsic (de-absorbed), rest-frame 2-10 keV luminosity is $\sim 2.5 \times 10^{44} \text{ erg s}^{-1}$, which places XID403 at the low end of the X-ray luminosity range for type-2 quasars. Admittedly, the uncertainties in the geometry of the obscuring (and reprocessing) material might substantially affect the derivation of the intrinsic luminosity. However, we note that, if the spectrum were produced by pure reflection and a typical reflection efficiency of $\sim 2\%$ is assumed (Gilli et al. 2007), the intrinsic luminosity would be even higher.

XID403 was detected in the 1 Ms CDFS catalog by Giacconi et al. (2002, XID=618), with $f_{0.5-2} = 1.6 \pm 0.5 \times 10^{-16} \text{ erg cm}^{-2} \text{ s}^{-1}$ and $f_{2-10} < 7.6 \times 10^{-16} \text{ erg cm}^{-2} \text{ s}^{-1}$. The ~ 4 times larger soft X-ray flux is likely due to contamination from high background fluctuations over the larger ($8''$ radius) extraction region adopted in

that catalog. We checked the photometry of the 2000, 2007 and 2010 periods separately using a smaller $3''$ radius: no significant source variability is detected in any band. XID403 was below the detection thresholds of the 1 Ms CDFS catalog by Alexander et al. (2003) and 2Ms CDFS catalogs by Luo et al. (2008).

4. DISCUSSION AND CONCLUSIONS

4.1. SED fitting

We searched for additional indicators of heavy obscuration by considering data at other wavelengths. We first investigated the observed (i.e., not corrected for absorption), rest-frame 2-10 keV to $6\mu\text{m}$ luminosity diagnostic ratio (X/IR, e.g., Alexander et al. 2008a). We derived the X-ray luminosity from the spectral fit and used the $\sim 4\mu\text{m}$ rest-frame luminosity (derived from the Spitzer/MIPS datapoint at $24\mu\text{m}$) as a proxy for the $6\mu\text{m}$ luminosity. The X/IR ratio of $\sim 5 \times 10^{-3}$ would place XID403 in the region populated by Compton-thick AGN (Alexander et al. 2008a). When considering the $F(24\mu\text{m})/F(R)$ vs $R - K$ color diagram elaborated by Fiore et al. (2009), XID403 would fall in “cell E”, where a significant fraction ($\sim 25 - 30\%$) of galaxies is found to host a heavily obscured, candidate Compton-thick AGN.

We then built the Spectral Energy Distribution (SED) from the X-rays to the radio regime (see Fig.2). As already shown by Coppin et al. (2009), the radio to FIR emission of this source is dominated by dusty star formation, at a rate of $\sim 1000 M_\odot \text{ yr}^{-1}$. We note that X-ray binaries associated to such a high SFR would produce $L_{2-10}^{obs} \sim 2 - 5 \times 10^{42} \text{ erg s}^{-1}$ (Ranalli et al. 2003; Lehmer et al. 2010), similar to the *observed* value. However, X-ray binaries have on average much softer spectra ($\Gamma \gtrsim 1.5$, Remillard & McClintock 2006) than observed ($\Gamma = -0.64$). If absorption is invoked to explain such a spectral hardness, then intrinsic luminosities of $\approx 10^{44} \text{ erg s}^{-1}$ are derived, which are incompatible with X-ray binary emission.

A reasonable match with the MIR to UV datapoints could be obtained with a reddened QSO template with $A_V \sim 0.7 - 0.8$ (adopting the extinction curve of Gaskell & Benker 2007). When converting the measured

¹⁵ When grouping to a minimum of 1 count per bin, the value of the C-statistic over the degrees of freedom is 54.7/59 and 55.2/60 for the *plcabs* and *pexrav* model, respectively.

optical extinction into an equivalent hydrogen column density by applying the relation valid for the Milky Way ISM ($N_H \sim 1.8 \times 10^{21} A_V$), we find $N_H \sim 1.3 \times 10^{21} \text{ cm}^{-2}$, which is three dex smaller than what is estimated from the X-ray spectral fit. A mismatch between the X-ray and the optically estimated column density, in the range of $\sim 3 - 100$, is observed in local AGN, calling for a number of interpretations (e.g., low dust-to-gas ratio; Maiolino et al. 2001). The mismatch observed in XID403 is ~ 1000 , which would make this object extreme.

In their SED analysis Coppin et al. (2009) suggest a different, stellar origin for the optical/UV rest frame emission. Following the parameterization used by Vignali et al. (2009) and Pozzi et al. (2010) for obscured AGN, we fitted the SED of XID403 with a stellar component, an AGN torus component, and a dusty starburst component. The dusty starburst is responsible for the bulk of the FIR to radio emission, while the AGN torus produces the entire emission at $24\mu\text{m}$ ($4\mu\text{m}$ rest-frame). A galaxy template with $M_* \sim 1.2 \times 10^{11} M_\odot$, $A_V \sim 1$ and a ~ 1 -Gyr-old constant star formation rate nicely fits the optical/UV_{rest} data. However, a possible problem in interpreting the optical/UV_{rest} emission as stellar light is that XID403 is pointlike in the deep HST/ACS images (CLASS_STAR=0.99 in i_{775} and z_{850}), which would imply a half-light radius of < 0.3 kpc. Although very compact morphologies have been observed in a fraction of distant sub-mm galaxies (Ricciardelli et al. 2010), the pointlike nature of XID403, coupled to the presence of broad NV emission, might suggest that the optical/UV_{rest} light has a nuclear origin. In particular, we could be looking at a fraction ($\sim 10\%$) of nuclear radiation that leaks out without being absorbed or is scattered towards us and thus would be polarized. If true, the effective extinction to the nucleus would be much higher than that estimated by fitting the whole MIR to UV emission with a reddened QSO template, being more in line with the large X-ray column density. This interpretation has been already proposed by Polletta et al. (2008) to explain the relatively blue optical/UV emission and broad line components of two sub-mm galaxies at $z \sim 3.5$ hosting heavily obscured AGN, similar to XID403. Also, although the stellarity parameter is uncertain for the faint K -band detection, the decrease of CLASS_STAR from 0.95 in Y to 0.74 in K may also suggest that the host galaxy contributes significantly only at $\lambda_{rest} > 4000\text{\AA}$. In Fig.2 we show a possible SED decomposition for XID403 obtained by adding an AGN torus component and a scattering component (corresponding to $\sim 10\%$ of the AGN intrinsic UV emission¹⁶) to the SED of Arp220. In summary, the full SED analysis shows that XID403 is not a classic, type-2 QSO (i.e., a narrow-line, X-ray obscured AGN whose physical properties can be explained within the standard, geometry-based Unified Model; Norman et al. 2002), but points to a complex physical picture likely related to its active assembly phase.

4.2. Black hole and stellar mass growth

¹⁶ The intrinsic AGN UV emission is estimated by normalizing the QSO template of Elvis et al. (1994) to the Spitzer/MIPS datapoint.

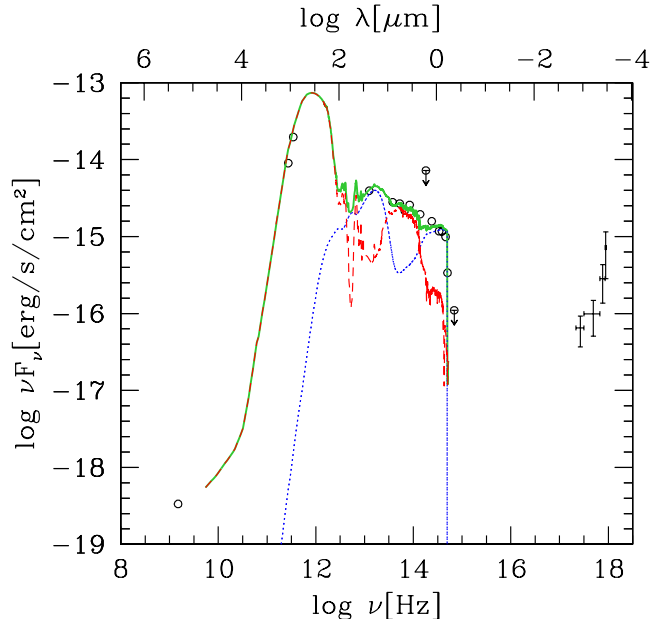


FIG. 2.— Spectral energy distribution of XID403 (observed frame) and possible decomposition into a galaxy component (red dashed line) and an AGN component (blue dotted line). The green solid line is the sum of the two. The template of Arp 220 shifted to $z = 4.76$ is adopted for the galaxy emission. The sum of a torus and a scattered component is adopted for the AGN emission (see text).

The IR emission from the AGN torus and the measured X-ray emission are used (see e.g., Vignali et al. 2009; Pozzi et al. 2010) to derive an AGN bolometric power of $7 \times 10^{45} \text{ erg s}^{-1}$. Assuming that the BH is radiating at the Eddington limit, as might be expected during these active BH and galaxy build-up phases, would imply $M_{BH} = 5 \times 10^7 M_\odot$. This in turn gives $M_{BH}/M_* \sim 4 \times 10^{-4}$, which is a factor of 5 smaller than the local value. It would then seem that both BH and stellar mass are rapidly growing towards their final values, but the BH is lagging behind as seen in sub-mm galaxies at $z \sim 2$ (Alexander et al. 2008b) and expected by recent semi-analytic models of BH/galaxy formation (Lamastra et al. 2010). However, since the estimated BH mass is a lower limit (accretion might be sub-Eddington) and the stellar mass derived in the previous section might be an upper limit (the AGN likely contributes to the optical/UV_{rest} light), this ratio might well be equal to the local value.

4.3. Expectations for high- z Compton-thick AGN

While the space density of luminous, unobscured and moderately obscured QSOs declines exponentially at $z \gtrsim 3$ (e.g., Brusa et al. 2009; Civano et al. 2011), the behaviour of heavily obscured objects has still to be properly determined. Semi-analytic models of BH/galaxy evolution linking the obscuration on nuclear scales to the gas availability in the host galaxy (e.g., Menci et al. 2008), would predict an increasing abundance of obscured AGN towards high redshifts, and some observational evidence of this trend has been reported (Treister et al. 2009 and references therein).

We considered the number of Compton-thick AGN as expected from the synthesis model by Gilli et al. (2007).

XID403 is detected with a 2-10 keV flux ~ 2 times larger than the detection limit at its position. The mean limiting flux over the 160 arcmin² GOODS-S area is $f_{2-10} = 1.5 \times 10^{-16}$ erg cm⁻² s⁻¹. Using the Gilli et al. (2007) model, one would expect from 0.06 to 0.6 Compton-thick AGN in the range of $4.7 < z < 5.7$ with $f_{2-10} > 3 \times 10^{-16}$ erg cm⁻² s⁻¹ in GOODS-S, depending on whether their space density undergoes the same high- z decline as observed for less obscured QSOs or stays nearly constant. Clearly, any firm conclusion is prevented by the low statistics. However, the mere presence of a Compton-thick AGN at $z > 4$ in such a small area (and this could be a lower limit since we did not investigate the whole X-ray source catalog) might suggest that the space density of Compton-thick AGN is not rapidly declining towards high redshifts. This shows that the detection of even a small number of heavily obscured AGN at $z > 4$ in ultra-deep X-ray surveys would have a strong leverage on our understanding of early BH evolution.

X-ray spectral analysis is the only unambiguous way to determine whether an AGN is shrouded by Compton-thick matter. Observations at energies above 10 keV are an obvious way to identify Compton-thick AGN, but the

current high-energy instrumentation and that foreseen in the near future (*NuSTAR*, *Astro-H*) will not allow sampling objects beyond $z \sim 1 - 1.5$. Below 10 keV, sensitive observations with limiting fluxes of $\approx 10^{-17}$ erg cm⁻² s⁻¹ over wide sky areas, such as those from the proposed missions *IXO* (White et al. 2010) and *WFXT* (Murray et al. 2010), would be required. The only concrete way to detect and unambiguously recognize high- z Compton-thick AGN in the near future is through even deeper observations with *Chandra*.

We acknowledge the following supporting agencies and grants: Italian Space Agency (ASI) under the ASI-INAF contracts I/009/10/0 and I/088/06/0 (RG, CV, AC); NASA through CXC grant SP1-12007A and ADP grant NNX10AC99G (WNB, YQX, BL); *Chandra* archival grant SP89004X (AP, RG); DFG cluster of excellence Origin and Structure of the Universe (PR). We thank the referee for a constructive report and N. Miller and M. Mignoli for useful discussions. RG gratefully acknowledges hospitality by the Johns Hopkins University where this work started.

REFERENCES

- Akylas, A., & Georgantopoulos, I. 2009, *A&A*, 500, 999
 Alexander, D. M., et al. 2003, *AJ*, 126, 539
 —. 2008a, *ApJ*, 687, 835
 —. 2008b, *AJ*, 135, 1968
 Bauer, F. E., Yan, L., Sajina, A., & Alexander, D. M. 2010, *ApJ*, 710, 212
 Brandt, W. N., Guainazzi, M., Kaspi, S., Fan, X., Schneider, D. P., Strauss, M. A., Clavel, J., & Gunn, J. E. 2001, *AJ*, 121, 591
 Brandt, W. N., & Hasinger, G. 2005, *ARA&A*, 43, 827
 Broos, P. S., Townsley, L. K., Feigelson, E. D., Getman, K. V., Bauer, F. E., & Garmire, G. P. 2010, *ApJ*, 714, 1582
 Brusa, M., et al. 2009, *ApJ*, 693, 8
 Cash, W. 1979, *ApJ*, 228, 939
 Castellano, M., et al. 2010, *A&A*, 524, A28+
 Civano, F., et al. 2011, *ApJ*, submitted
 Comastri, A. 2004, in *Astrophysics and Space Science Library*, Vol. 308, *Supermassive Black Holes in the Distant Universe*, ed. A. J. Barger, 245–+
 Comastri, A., et al. 2011, *A&A*, 526, L9+
 Coppin, K. E. K., et al. 2009, *MNRAS*, 395, 1905
 —. 2010, *MNRAS*, 407, L103
 Daddi, E., et al. 2007, *ApJ*, 670, 173
 Elvis, M., et al. 1994, *ApJS*, 95, 1
 Fabian, A. C. 1999, *MNRAS*, 308, L39
 Feruglio, C., Daddi, E., Fiore, F., Alexander, D. M., Piconcelli, E., & Malacaria, C. 2011, *ArXiv e-prints*
 Fiore, F., et al. 2009, *ApJ*, 693, 447
 Gaskell, C. M., & Benker, A. J. 2007, *ArXiv e-prints*
 Giacconi, R., et al. 2002, *ApJS*, 139, 369
 Giavalisco, M., et al. 2004, *ApJ*, 600, L93
 Gilli, R., Comastri, A., & Hasinger, G. 2007, *A&A*, 463, 79
 Lamastra, A., Menci, N., Maiolino, R., Fiore, F., & Merloni, A. 2010, *MNRAS*, 405, 29
 Lehmer, B. D., Alexander, D. M., Bauer, F. E., Brandt, W. N., Goulding, A. D., Jenkins, L. P., Ptak, A., & Roberts, T. P. 2010, *ApJ*, 724, 559
 Luo, B., et al. 2008, *ApJS*, 179, 19
 Maiolino, R., Marconi, A., & Oliva, E. 2001, *A&A*, 365, 37
 Marconi, A., Risaliti, G., Gilli, R., Hunt, L. K., Maiolino, R., & Salvati, M. 2004, *MNRAS*, 351, 169
 Menci, N., Fiore, F., Puccetti, S., & Cavaliere, A. 2008, *ApJ*, 686, 219
 Murphy, K. D., & Yaqoob, T. 2009, *MNRAS*, 397, 1549
 Murray, S. S., et al. 2010, in *Presented at the Society of Photo-Optical Instrumentation Engineers (SPIE) Conference*, Vol. 7732, *Society of Photo-Optical Instrumentation Engineers (SPIE) Conference Series*
 Norman, C., et al. 2002, *ApJ*, 571, 218
 Oesch, P. A., et al. 2007, *ApJ*, 671, 1212
 Polletta, M., et al. 2008, *A&A*, 492, 81
 Pozzi, F., et al. 2010, *A&A*, 517, A11+
 Ranalli, P., Comastri, A., & Setti, G. 2003, *A&A*, 399, 39
 Remillard, R. A., & McClintock, J. E. 2006, *ARA&A*, 44, 49
 Ricciardelli, E., Trujillo, I., Buitrago, F., & Conselice, C. J. 2010, *MNRAS*, 406, 230
 Risaliti, G., Maiolino, R., & Salvati, M. 1999, *ApJ*, 522, 157
 Su, J., et al. 2011, *ApJ*, submitted
 Teplitz, H. I., et al. 2011, *AJ*, 141, 1
 Tozzi, P., et al. 2006, *A&A*, 451, 457
 Treister, E., Urry, C. M., & Virani, S. 2009, *ApJ*, 696, 110
 Vanzella, E., et al. 2006, *A&A*, 454, 423
 Vignali, C., et al. 2009, *MNRAS*, 395, 2189
 White, N. E., Parmar, A., Kunieda, H., Nandra, K., Ohashi, T., & Bookbinder, J. 2010, in *American Institute of Physics Conference Series*, Vol. 1248, *American Institute of Physics Conference Series*, ed. A. Comastri, L. Angelini, & M. Cappi, 561–566
 Xue, Y. Q., et al. 2011, *ApJS*, submitted
 Yaqoob, T. 1997, *ApJ*, 479, 184